IMAGING MEMBRANE PROTEINS IN THEIR NATIVE ENVIRONMENT WITH THE ATOMIC FORCE MICROSCOPE

Andreas Engel, Frank A. Schabert, Daniel J. Müller, and Christian Henn
M. E. Müller-Institute for Microscopic Structural Biology,
Biozentrum, University of Basel, Klingelbergstr. 70
CH-4056 Basel, Switzerland

ABSTRACT. Two well-characterized regular membrane protein arrays are imaged in aqueous solutions with the atomic force microscope (AFM). The interpretation of these topographs is discussed in terms of data from EM and x-ray crystallography.

1. Introduction

To understand the function of biomolecules and their supramolecular assemblies, a precise knowledge of their structure is a prerequisite. X-ray crystallography has so far been the most successful technique to establish the atomic structure of biomolecules. It requires the availability of highly ordered 3D crystals, as well as heavy metal derivatives thereof. This is a major hurdle for the structural analysis of membrane proteins, as these need to be extracted from the bilayer by detergents for purification. Frequently, membrane proteins are not stable under such conditions, preventing successful 3D crystallization.

However, membrane proteins have been reconstituted into lipid bilayers to restore and assess their biological activity. In addition, some membrane proteins have been reconstituted into 2D lattices in the presence of phospholipids (Jap, et al., 1992). Electron crystallography initially developed to solve the structure of bacteriorhodopsin (Henderson, et al., 1990) has been successfully used to analyze the structure of light harvesting complex (LHC) at atomic scale resolution (Kühlbrandt, et al., 1994).

In addition, significant progress has been achieved in the analysis of biomolecular structures with the AFM. After initial experiments with the purple membrane documenting the potential of this scanning probe instrument to achieve high resolution on soft surfaces (Butt, et al., 1990), different avenues have been pursued. First, techniques have been developed to immobilize samples for imaging in buffer solutions using the contact mode of the AFM (Karrasch, et al., 1993, Wagner, et al., 1994). Second, the tapping mode has been applied to scan surfaces in solution (Hansma, et al., 1994), providing powerful possibilities to image biomolecules that are not strongly attached to a substrate (Bezanilla, et al., 1994, Radmacher, et al., 1994) as well as soft cells (putman, et al., 1994). Third, the reproducibility of AFM data acquired at subnanometer resolution has been demonstrated (Schabert and Engel, 1994), and their accuracy by comparison with data from electron microscopy (Karrasch, et al., 1994, Müller D. J., et al., 1995a) as well as X-ray crystallography has been assessed (Schabert, et al., 1995). Furthermore, recent results suggest that the AFM may indeed become an important tool to monitor conformational changes of membrane protein surfaces at close to atomic scale resolution (Müller D. J., et al., 1995b, Schabert, et al., 1995).

As resolution and reproducibility increase, the question whether the imaging process may be understood in its full complexity should be addressed. Tip sample interactions have been modeled at atomic scale (Cicarci, et al., 1992), but biological surfaces are too complex for an elegant application of such models. Long range (3 - 30 Å) weak van der Waals attractions, and strong electrostatic interactions, as well as short range (< 1 Å) shell-shell repulsion need to be considered. They depend on the specific physico-chemical properties of both tip and sample surfaces, and of the solutes in the aqueous environment. Since the stylus is much stiffer than the biological structure, the viscoelastic properties of the latter are likely to have a dominant influence on the image acquired with the AFM.

Experimental studies have revealed the influence of pH and ionic strength on tip-sample interaction forces (Butt, 1991). Viscoelasticity has been investigated at large scale (Radmacher, et al., 1993), but no analysis has yet been reported at submolecular scale resolution.

As a preliminary step towards a better understanding of the imaging process in the AFM we compare model images calculated with various tip shapes from the atomic scale model of 2D OmpF lattices (Schabert, et al., 1995) with the experimental data. Further, we discuss dynamic changes of the bacteriorhodopsin surfaces resulting from tip-sample interactions (Müller D. J., et al., 1995b).

2. Imaging a regular protein layer in buffer solution with the AFM

Fig. 1 displays the extracellular surface of a 2D rectangular type crystal (a = 135 Å, b = 82 Å) assembled from E. coli OmpF porin trimers in the presence of lipids (Hoenger, et al., 1990) as recorded with the AFM in buffer solution. The crystals have been adsorbed to freshly cleaved mica in the presence of Mg^{2+}. According to the diffraction pattern (Fig. 1, top right) the lateral resolution is 13 Å. High resolution has been achieved reproducibly by optimization of the recording conditions. Critical were the state of the tip, the scan speed, and the force (Schabert and Engel, 1994). Specifically, this corrugated surface exhibiting protein domains protruding by 12 Å from the bilayer surface required the force to be reduced to underlined approximately 100 pN for repeated acquisition of high resolution topographs.
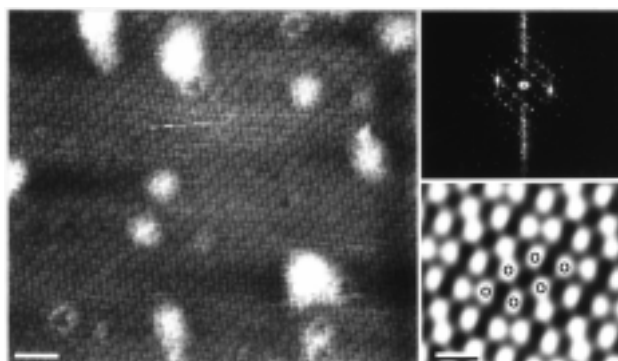

Figure 1. The extracellular surface of OmpF porin recorded with a Nanoscope III (Digital Instruments, Santa Barbara, Ca, USA) and oxide sharpened Si_3N_4 tips on a 100 μm long cantilever with a spring constant $k = 0.1$ N/m (Olympus Ltd., Japan). In the top right inset the diffraction pattern is displayed. Diffraction orders extend to a resolution of 13 Å. The average shown in the lower right corner exhibits trenches that run from the lower left to the upper right corner. One set of trimers is marked. Scale bars represent 300 Å in A) and 60 Å in B).

3. Interpretation of high resolution topographs recorded with the AFM

The quality of the topographic information prompted us to analyze the reproducibility by calculation of the standard deviation maps from sets of aligned porin trimer images (Schabert and Engel, 1994). In addition, an atomic scale model of the 2D crystal was assembled with the atomic OmpF structure from X-ray crystallography (Cowan, et al., 1992), and the topographs recorded with the AFM (Schabert, et al., 1995). Fig. 2 documents the close fit between the atomic model rendered to 15 Å resolution and the topography from the AFM. A precise determination of the lipid surface contour was achieved on the periplasmic side. This information allowed the lipid bilayer to be modeled at atomic scale (Schabert, et al., 1995), providing new experimental evidence on the interaction between lipids and membrane proteins.
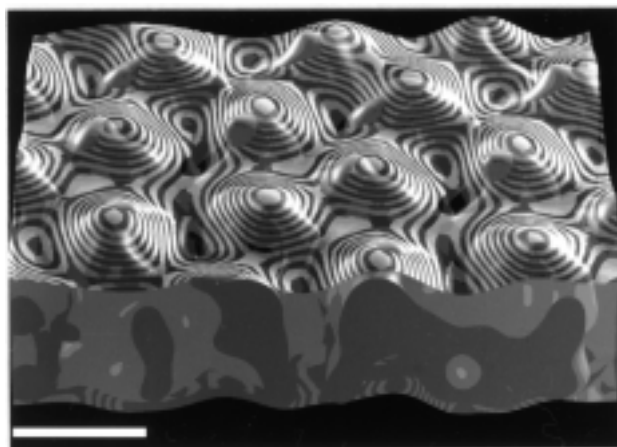
Figure 2. Comparison of the extracellular porin surface topography recorded with the AFM with the atomic scale model calculated from the atomic structure of the porin trimer (Cowan, et al., 1992). Experimental data are contoured, while the protein model is rendered at 15 Å resolution in gray shades. In some cases, the model breaks through the experimental surface, suggesting a deformation of the protein that is likely to result from the force exerted by the stylus. The vertical distance between bright contours is 1 Å , and the scale bar is 50 Å
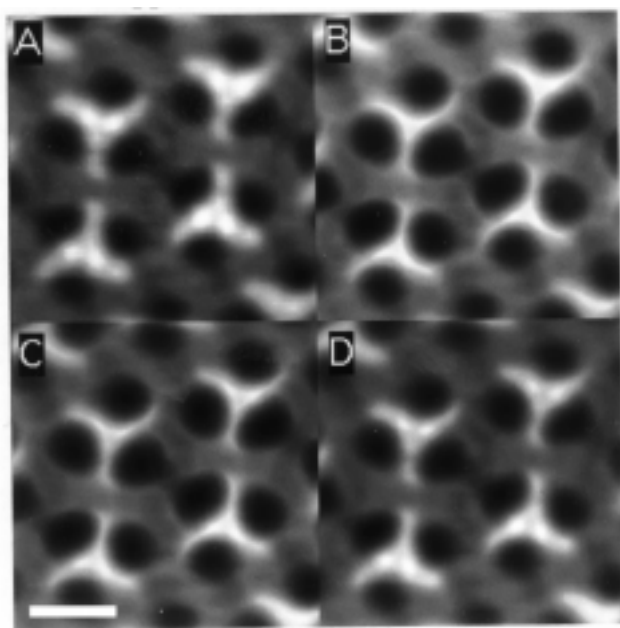

Figure 3. Reconstruction of the periplasmic OmpF porin topography with different tip models. A) Average of the raw data. B) Reconstruction of the average with a parabolic tip (r = 9 Å). C) Reconstruction with a rounded cone tip (cone angle $\alpha = 20°$, and tip radius r = 9 Å). D) Reconstruction with a parabolic tip (r = 3 Å). Scale bar is 50 Å.

With the atomic model of the OmpF porin crystal the validity of surface reconstruction algorithms (Keller and Franke, 1993) can be assessed. According to an approximate estimate, the cantilevers used to record images such as shown here had tip radii of 20 Å (Schabert and Engel, 1994). The reconstructions displayed in Fig. 3 reveal the dilemma in determining the tip parameters: if tip models are used that have a reasonable shape (i.e., $r \geq 9$ Å; Figs. 3B and 3C), the reconstructed topographs exhibit sharp features that have not much in common with the atomic structure of the periplasmic porin surface (see Fig. 4A). However, to calculate reconstructions that exhibit a satisfactory similarity with the atomic structure, rather unrealistic tip radii $r \leq 3$ Å have to be assumed (Fig. 3D). These results suggest that the present geometrical reconstruction methods need to be expanded to become applicable to the reconstruction of soft
biological surfaces.

We have also evaluated whether a convincing simulation of the raw data can be achieved with hard surface models using a rounded cone, a cylindrical, and a parabolic tip. Fig. 4 documents that none of the tip shapes tested led to a satisfactory result. In all cases, the simulated image exhibited marked differences compared to the raw data, although general features and the apparent depth of the channels were properly reproduced. When the atomic scale model is simply rendered at 8 Å resolution (Fig. 4B)

however, its features resemble those of the image recorded with the AFM (Fig. 3A). In conclusion, hard surface models that simulate the shell-shell repulsion, appear to be unsuitable for modeling image formation in the AFM. Such approaches do neither account for the elasticity of the structure being palpated nor the long range forces.
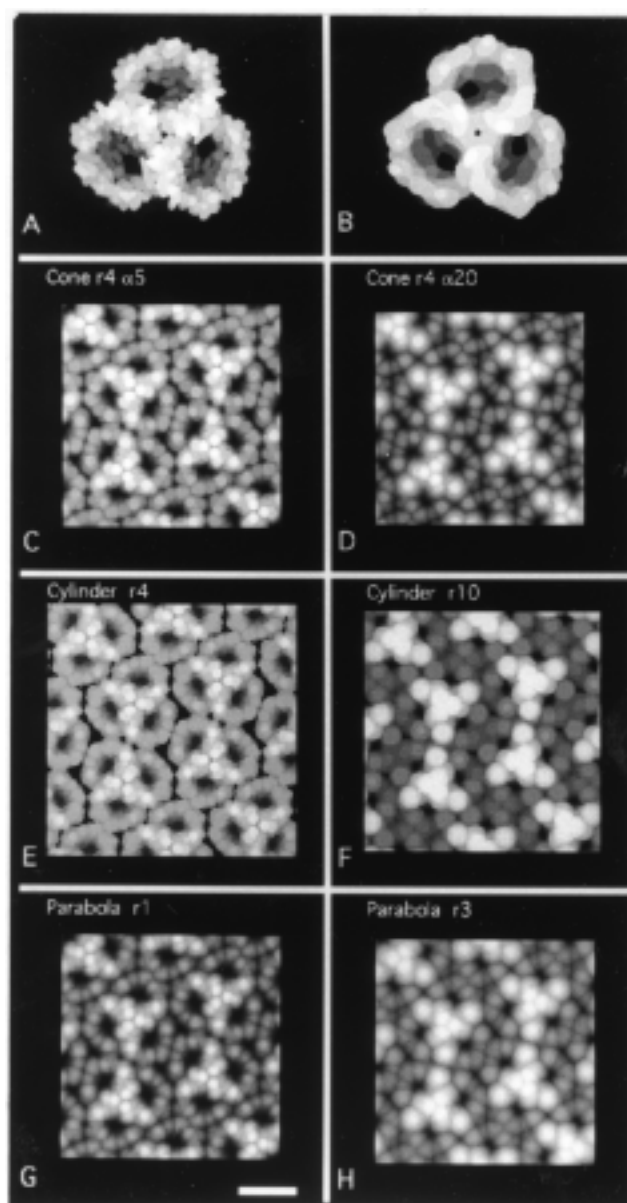

Figure 4. Simulation of OmpF porin topographs. A) The periplasmic surface rendered at 2 Å resolution. B) The periplasmic surface rendered at 8 Å resolution. C) Convolution with a rounded cone tip (cone angle α = 5° and tip radius r = 4 Å). D) Convolution with a rounded cone tip (cone angle α = 20° and tip radius r = 4 Å). E) Convolution with a cylindrical tip (tip radius r = 4 Å). F) Convolution with a cylindrical tip (tip radius r = 10 Å). G) Convolution with a parabolic tip (tip radius r = 1 Å). H) Convolution with a parabolic tip (tip radius r = 3 Å). Scale bar is 50 Å.

4. Force induced conformational changes

Molecular interaction forces have recently been measured to some 100 pN (Dammer, et al., 1995, Florin, et al., 1994, Lee, et al., 1994, Moy, et al., 1994). Therefore, it is likely that the finest protein structures we can detect with the AFM undergo conformational changes when loaded with forces of that order. Indeed, as mentioned above, reproducible imaging of the extracellular porin surface requires imaging forces of approximately 100 pN. Two questions emerge: First, are tip-induced conformational changes reversible, and second, what are typically the smallest structures that can

reproducibly be imaged in their 'native' conformation? Recent experiments with the purple membrane may provide some answers. Two conformations have been observed on the cytoplasmic surface of bacteriorhodopsin which we interpreted as a force dependent conformational change of the polypeptide connecting the helices E and F (Müller D. J., et al., 1995b). Furthermore, the stiffness of this loop has been found to depend on the pH, high values increasing the stability. It has therefore been speculated that electrostatic interactions are likely to stabilize this loop. As Fig. 5 demonstrates, a slight force variation during the scan profoundly changes the morphology of the bacteriorhodopsin trimers. The effect is fully reproducible: by reducing the force, trimeric sharp protrusions emerge, whereas bacteriorhodopsin trimers exhibit a donut-like surface when the force is increased. This can be observed over several scans, imaging always the same area, provided that the force is $\leq$ 500 pN.

OmpF porin and bacteriorhodopsin both suggest that the critical loading force is approximately 100 pN. Apparently, single polypeptide loops remain close to their native conformation when imaged in contact mode with instruments that allow stable operation at such low forces. The reversibility and small energy required to induce the change (approximately 6 kcal/mol; Müller D. J., et al., 1995b) indicate that the imaging process does not induce structural damage.

5. Conclusions

Progress in imaging soft biological samples with the AFM in their native environment at high resolution suggests that this instrument is a powerful tool for the structural biologist. The information acquired is complementary to that obtained by all other techniques presently known. Of particular interest are the possibilities to extract surface features of the biomolecules with a vertical resolution of about 1 Å, and to monitor conformational changes at subnanometer lateral resolution. 100 pN appears to be a critical limit of the loading force when protruding single polypeptide loops are to be imaged. As this is also close to the practical limitation in the operation of current commercial instruments, developments to reduce the loading force would be desirable. Further, the atomic model of the 2D OmpF porin/lipid crystal discussed here may serve as a basis to improve reconstruction algorithms that account for long range forces and the viscoelasticity of the sample.
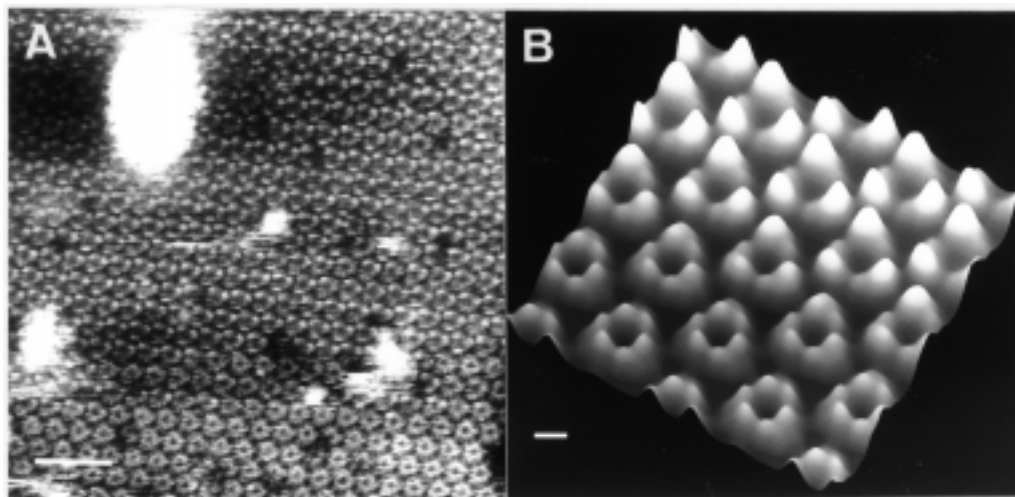

Figure 5. Conformational changes of bacteriorhodopsin. A) The unprocessed image has been recorded with forces of approximately 100 pN at the top, whereas the force has been increased to 300 pN at the bottom of the scan. B) Averages from images recorded at a force of 100 pN, and averages from images recorded at 300 pN have been merged to a composite image displaying the force induced conformational change. Scale bars are 200 Å in A) and 20 Å in B).

6. Acknowledgement

7. References

Bezanilla, M., Drake, B., Nudler, E., Kashlev, M., Hansma, P. K. & Hansma, H. G. (1994). Motion and Enzymatic Degradation of DNA in the Atomic Force Microscope. *Biophys. J.* **67**, 2454-2459.

Butt, H.-J., Downing, K. H. & Hansma, P. K. (1990). Imaging the membrane protein bacteriorhodopsin with the atomic force microscope. *Biophys. J.* **58**, 1473-1480.

Butt, H.-J. (1991). Measuring Electrostatic, van der Waals, and Hydration Forces in Electrolyte Solutions with an Atomic Force Microscope. *Biophys.J.* **60**, 1438-1444.

Cicarci, S., Tekman, E. & Baratoff, A. (1992). Theoretical study of short- and long-range forces and atom transfer in scanning force microscopy. *Physical Rev. B* **46**, 10411-10422.

Cowan, S. W., Schirmer, T., Rummel, G., Steiert, M., Ghosh, R., Pauptit, R. A., Jansonius, J. N. & Rosenbusch, J. P. (1992). Crystal structures explain functional properties of two E. coli porins. *Nature* **358**, 727-733.

Dammer, U., Popescu, 0., Wagner, P., Anselmetti, D., Güntherodt, H. J. & Misevic, G. N. (1995). Binding strength between cell adhesion proteoglycans measured by atomic force microscopy. *Science* **267**, 1173-1175.

Florin, E. L., Moy, V. T. & Gaub, H. E. (1994). Adhesion Forces Between Individual Ligand-Receptor Pairs. *Science* **264**, 415-417.

Hansma, P. K., Cleveland, J. P., Radmacher, M., Walters, D. A., Hillner, P., Bezanilla, M., Fritz, M., Vie, D. & Hansma, H. G. (1994). Tapping Mode Atomic Force Microscopy in Liquids. *Appl. Phys. Let.* **64**, 1738-1740.

Henderson, R., Baldwin, J. M., Ceska, T. A., Zemlin, F., Beckmann, E. & Downing, K. H. (1990). Model for the structure of bacteriorhodopsin based on high-resolution electron cryo-microscopy. *J. Mol. Biol.* **213**, 899-929.

Hoenger, A., Gross, H., Aebi, U. & Engel, A. (1990). Localization of the lipolysaccharides in metalshadowed reconstituted lipid-porin membranes. *J. Struct. Biol.* **103**, 185-195.

Jap, B. K., Zulauf M., Scheybani, T., Hefti, A., Baumeister, W. & Aebi, U. (1992). 2D crystallization: from art to science. *Ultramicroscopy* **46**, 45-84.

Karrasch, S., Dolder, M., Schabert, F., Ramsden, J. & Engel, A. (1993). Covalent binding of biological samples to solid supports for scanning probe microscopy in buffer solution. *Biophys. J.* **65**, 2437-2446.

Karrasch, S., Hegerl, R., Hoh, J. H., Baumeister, W. & Engel, A. (1994). Atomic Force Microscopy

Produces Faithful High-Resolution Images of Protein Surfaces in an Aqueous Environment. *Proc. Natl. Acad.. Sci.* USA **91**, 836-838.

Keller, D. & Franke, F. (1993). Envelope reconstruction of probe microscope images. *Surface Science* **294**, 409-419.

Kühlbrandt, W., Wang, D. N. & Fujiyoshi, Y. (1994). Atomic Model of Plant Light-Harvesting Complex by Electron Crystallography. *Nature* **367**, 614-621.

Lee, G. U., Kidwell, D. A. & Colton, R. J. (1994). Sensing Discrete Streptavidin-Biotin Interactions with Atomic Force Microscopy. *Langtnuir* **10**, 354-357.

Moy, V. T., Florin, E. L. & Gaub, H. E. (1994). Intermolecular forces and energies between ligands and receptors. *Science* **266**, 257-259.

Müller D. J., Schabert, F. A., Büldt, G. & Engel, A. (1995a). Imaging bacteriorhodopsin molecules in aqueous solutions at subnanometer resolution using atomic force microscopy. *Biophys. J.* in press.

Müller D. J., Büldt, G. & Engel, A. (1995b). Force-induced conformational change of bacteriorhodopsin. *J. Mol. Biol.* in press.

Putman, C. A. J., van der Werf, K. O., de Grooth, B. G., van Hulst, N. F. & Greve, J. (1994). Viscoelasticity of living cells allows high resolution imaging by tapping mode atomic force micrscopy. *Biophys. J.* **67**, 1749-1743.

Radmacher, M., Fritz, M., Hansma, H. G. & Hansma, P. K. (1994). Direct observation of enzyme activity with the atomic force microscope. *Science* **265**, 1577-1579.

Radmacher, M., Tilmann, R. W. & Gaub, H. E. (1993). Imaging Viscoelasticity by Force Modulation with the Atomic Force Microscope. *Biophys. J* **64**, 735-742.

Schabert, F. A. & Engel, A. (1994). Reproducible acquisition of E. coli porin surface topographs by atomic force microscopy. *Biophys. J.* **67**, 2394-2403.

Schabert, F. A., Henn, C. & Engel, A. (1995). Native Escherichia Coli OmpF Porin Surfaces Probed by the Atomic Force Microscope. *Science* in press.

Wagner, P_ Kernen, P., Hegner, M., Ungewickell, E. & Semenza, G. (1994). Covalent anchoring of proteins onto gold-directed NHS-terminated self-assembled monolayers in aqueous buffers: SFM images of clathrin cages and triskelia. *FEBS letters* **356**, 267-271.